Mon. Not. R. Astron. Soc. **318**, 511–525 (2000)

Delta Scuti Network observations of XX Pyx: detection of 22 pulsation modes and of short-term amplitude and frequency variations

G. Handler,[1,2]★ T. Arentoft,[3] R. R. Shobbrook,[4,5] M. A. Wood,[6] L. A. Crause,[7] P. Crake,[8] F. Podmore,[9]† A. Habanyama,[10]† T. Oswalt,[6] P. V. Birch,[8] G. Lowe,[8] C. Sterken,[3] P. Meintjes,[11] J. Brink,[11]† C. F. Claver,[12] R. Medupe,[2,7] J. A. Guzik,[13]‡ T. E. Beach,[14]‡ P. Martinez,[2] E. M. Leibowitz,[15] P. A. Ibbetson,[15] T. Smith,[8] B. N. Ashoka,[16] N. E. Raj,[16] D. W. Kurtz,[7] L. A. Balona,[2] D. O'Donoghue,[2] J. E. S. Costa[17]§ and M. Breger[1]

[1]*Institut für Astronomie, Universität Wien, Türkenschanzstraße 17, A-1180 Wien, Austria*
[2]*South African Astronomical Observatory, PO Box 9, Observatory 7935, South Africa*
[3]*Vrije Universiteit Brussel, Pleinlaan 2, B-1050 Brussels, Belgium*
[4]*PO Box 518, Coonabarabran, NSW 2357, Australia*
[5]*Research School of Astronomy and Astrophysics, Australian National University, Weston Creek PO, ACT 2611, Australia*
[6]*Department of Physics and Space Sciences & SARA Observatory, Florida Institute of Technology, 150 W. Univ. Blvd., Melbourne, FL 32901, USA*
[7]*Department of Astronomy, University of Cape Town, Rondebosch 7700, South Africa*
[8]*Perth Observatory, Walnut Rd., Bickley, Western Australia 6076, Australia*
[9]*Department of Physics, University of Zimbabwe, PO Box MP167, Mount Pleasant, Harare, Zimbabwe*
[10]*Department of Physics, University of Zambia, PO Box 32379, Lusaka, Zambia*
[11]*Physics Department, University of the Orange Free State, Bloemfontein 9300, South Africa*
[12]*National Optical Astronomy Observatories, PO Box 26732, Tucson, Arizona 85726-6732, USA*
[13]*Los Alamos National Laboratory, X-2, MS B220, Los Alamos, NM 87545-2345, USA*
[14]*Department of Natural Sciences, University of New Mexico, Los Alamos, 4000 University Drive, Los Alamos, NM 87544, USA*
[15]*Wise Observatory, Sackler Faculty of Exact Sciences, Tel Aviv University, Tel Aviv 69978, Israel*
[16]*Indian Space Research Organisation, Technical Physics Division, ISRO Satellite Centre, Airport Road, Bangalore 560017, India*
[17]*Instituto de Fisica, Universidade Federal do Rio Grande do Sul, 91501-970 Porto Alegre-RS, Brazil*

Accepted 2000 June 5. Received 2000 May 26; in original form 2000 March 15

ABSTRACT

We report multisite observations devoted to the main-sequence δ Scuti star XX Pyx, conducted as the 17th run of the Delta Scuti Network. Over 125 nights a total of 550 h of usable time-series photometric *B*- and *V*-filter data were acquired involving both photoelectric and CCD measurements at eight observatories spread around the world, which represents the most extensive single time-series for any pulsating star other than the Sun obtained so far.

We describe our observations and reduction methods, and present the frequency analysis of our new data. First, we detect six new pulsation and five new combination frequencies in the star's light curves. We also discover evidence for amplitude and/or frequency variations of some of the modes during the observations. These can occur on time-scales as short as 20 d and show quite diverse behaviour. To take them into account in the frequency analysis, a so-called non-linear frequency analysis method was developed, allowing us to quantify the temporal variability of the modes and to compensate for it. Following that we continue the frequency search and we also incorporate published multisite observations. In this way, we reveal three more pulsation and two more combination frequencies. In the end, we report a total of 30 significant frequencies – 22 of which correspond to independent pulsation modes. This is the largest number of independent modes ever detected in the light curves of a δ Scuti star.

★ E-mail: gerald@saao.ac.za
† SAAO Summer School student.
‡ Guest observer, McDonald Observatory, University of Texas at Austin, USA.
§ Guest observer, Laboratorio Nacional de Astrofisica/CNPq, Brazil.

The frequencies of the modes show preferred separations as already suggested by previous work on this star; they are also arranged in clear patterns. These results lead to a refinement of the stellar mean density ($\bar{\rho} = 0.241 \pm 0.008\,\bar{\rho}_{\odot}$) and to a new constraint on the rotation rate of XX Pyx ($\nu_{\rm rot} = 1.1 \pm 0.3\,{\rm d}^{-1}$). However, our attempts to identify the modes by pattern recognition failed. Moreover, mode identification from multicolour photometry failed as well because the high pulsation frequencies make this method unfavourable. The diverse behaviour of the amplitude and frequency variations of some of the modes leaves resonances as the only presently known possibility for their explanation.

Key words: techniques: photometric – stars: individual: CD-24 7599 – stars: individual: XX Pyx – stars: oscillations – δ Scuti.

1 INTRODUCTION

Asteroseismology is the study of the interior structure of multiperiodically pulsating variable stars by identifying all the observed pulsation modes and by reproducing the observed frequency spectra via model calculations. With this method a good understanding of the interior structure of the Sun and of pulsating white dwarfs has been obtained. However, the application of asteroseismological techniques to main-sequence pulsators other than the Sun has proven to be difficult.

The most promising candidates for exploring the deep interior of main sequence stars through asteroseismology are the δ Scuti stars. These are spectroscopically (mostly) normal A–F stars of luminosity classes III–V; most of them are multiperiodic non-radial pulsators. Regrettably, seismological studies of these objects are not straightforward. The main problems are:

(i) Most of the excited pulsation modes have low photometric amplitude; a large amount of data is required to detect them (e.g. see Breger et al. 1999).

(ii) δ Scuti stars are low radial order p- and g-mode pulsators; asymptotic theory in general cannot be applied to decipher the pulsation spectra.

(iii) Many well-observed δ Scuti stars are in the phase of shell hydrogen burning; theoretical frequency spectra of such evolved δ Scuti stars are very dense. It is therefore difficult to identify the pulsation modes correctly as only a small percentage of unstable modes is actually observed (Dziembowski & Krolikowska 1990).

(iv) Most multiperiodic δ Scuti stars are fast rotators: rotationally split multiplets may overlap in frequency and second-order effects destroy equal frequency splittings (see Templeton, Bradley & Guzik 2000 for an illustration). Differential rotation would result in a further complication of the frequency spectrum.

(v) Mode identification methods usually have different sensitivities for different types of mode; they are therefore hard to cross-calibrate. Their reliability is often questionable and depends on the physical parameters of the target star (e.g. Balona & Dziembowski, private communication).

One possible way to overcome all these difficulties is to select stars with the simplest interior structure, slow rotation, and a large number of excited and detectable pulsation modes for in-depth studies. This idea is based on an examination of models of δ Scuti stars in the beginning of main-sequence evolution: the unstable mode spectrum of such models only comprises p-modes and is therefore relatively simple. If a sufficient number of these modes is detected in a real star, and if several consecutive radial overtones are excited, obvious patterns within the mode frequencies should appear, even if rotationally split multiplets of modes of different degree, ℓ, overlap. These patterns will allow an assignment of the pulsational quantum numbers ℓ and m to the modes (if the star obeys the same physics as the models). This method has been tested successfully (Handler 1998). Furthermore, photometric colour information could be used to check these mode identifications.

An ideal target for the application of this strategy is XX Pyx. Using 220 h of measurement during two Whole Earth Telescope (WET, Nather et al. 1990) campaigns, Handler et al. (1996, 1997) detected 13 pulsation frequencies in the light curves; this corresponds to approximately 40 per cent of the theoretically predicted number of modes with $\ell \leq 2$. For this low $v \sin i$ ($52\,{\rm km\,s^{-1}}$) δ Scuti star, Handler et al. (1997, hereafter HPO) managed to obtain some initial seismological results despite the lack of definite mode identifications: XX Pyx is a 1.85-$M_{\odot}$ star in the first half of its main-sequence evolution. A first seismological distance to a δ Scuti star of 650 ± 70 pc has been derived for this object. Pamyatnykh et al. (1998) attempted to obtain a 'best seismic model' for the star, but they could not find even one model that matched all the observed frequencies acceptably well. The reason for this result was suspected to be due to deficiencies in the model physics; the detection of more pulsation modes is hoped to point towards the cause of the problem.

XX Pyx is just sufficiently evolved that it may have one (and only one!) mode with g-mode properties in the interior excited. This particular mode can be used to determine the star's interior rotation rate and to measure the amount of convective core overshooting (Dziembowski & Pamyatnykh 1991), because a large fraction of this mode's kinetic energy originates from the outer part of the convective core. The size of the overshooting parameter is one of the most ill-determined quantities in stellar model calculations: it is 'found small if supposed small, large if supposed large' (Renzini 1987). A determination of this parameter is of crucial importance for the understanding of stellar structure and evolution, in particular for modelling open cluster HR diagrams (some people need convective overshooting to explain them), solar and stellar activity (the underlying dynamo mechanism) and, of course, stellar interiors.

Finally, XX Pyx has been reported to exhibit amplitude variations on time scales as short as one month, as well as frequency variability detectable over a few years (Handler et al. 1998, hereafter HPZ). This behaviour can make different sets of normal modes detectable at different times. Then the combined

ensemble of modes can be used for an asteroseismological investigation. Such a strategy has been applied successfully already (Bond et al. 1996, Kleinman et al. 1998).

For all the reasons stated above, we deemed it worthwhile to devote a large observational effort to XX Pyx. A major multisite campaign has therefore been organized by the Delta Scuti Network (see Zima 1997); the initial results of that campaign are the subject of this paper.

2 OBSERVATIONS

Our multisite photometry was carried out between 1998 January 15 and April 5; the total time-base of our data set is therefore 81 d. We used 13 different telescope/detector combinations at nine observatories suitably spread in geographic longitude, and we obtained data during 125 clear nights at the different sites. We utilized both charge-coupled devices (CCDs) and photomultipliers (PMTs) as detectors, taking advantage of their different wavelength sensitivities: CCD measurements were taken through the Johnson (or Bessell) *V* filter whereas the PMT observations were acquired through the Johnson *B* filter. A brief synopsis of our measurements is given in Table 1, where PMT1 denotes a single-channel photometer, PMT2 a two-channel photometer and PMT3 a three-channel photometer.

The photoelectric observations were taken as high-speed photometric measurements, i.e. continuous 10-s integrations on the target star were performed. Because of the faintness of XX Pyx ($V = 11.50$ mag) and its short periods, this is the observing technique which promises the best results (see Handler 1995 for a more detailed discussion) in the case of photoelectric observations. The integrations on the target star were only interrupted to acquire measurements of sky background. If single-channel photometers were employed, additional observations of a close comparison star (SAO 176755) were obtained at hourly intervals. For multi-channel photometers, the latter object served as a sky-transparency monitor in Channel 2.

Our CCD measurements were obtained with a number of 512×512 and 1024×1024 chips, resulting in fields of view between 3×3 and 11×11 arcmin^2. The telescopes were pointed to acquire the maximum number of possible comparison stars on the frames, and care was taken to minimize drifts of the images over the chip. Integration times were chosen to yield one image every 60–120 s. Bias and dark frames as well as sky or dome flat fields were also taken every night (whenever possible).

3 REDUCTIONS

3.1 Initial CCD reductions; variable stars in the field

The reduction of the CCD frames was started by correcting for bias and flat field using standard routines. For the SARA observations, a correction for dark current was also useful. The extraction of the stellar time series was mainly accomplished using the MOMF package (Kjeldsen & Frandsen 1992), which combines point spread function (PSF)-fitting and aperture photometric techniques and gives excellent results. Under some circumstances (e.g. slow image rotation during a run) this needed to be supplemented by IRAF aperture photometry. The MOMF routines allow an easy choice of optimal aperture sizes, whereas we followed Handler, Kanaan & Montgomery (1997) for determining the best aperture radii for the IRAF results. The SAAO CCD measurements were analyzed using a modified version of DoPhot; the results were compared to those obtained by MOMF and found to be of similar quality.

We took special care in checking the constancy of the CCD comparison stars; we found two new variable stars in the field. A finding chart for those stars is given in Fig. 1. Variability of Star A ($V = 15.1$, no identification found in the literature) was discovered on the SAAO CCD frames. It varied sinusoidally with a time-scale of about 20 d and an amplitude of about 0.1 mag. The new variable *B* (GSC 6589-0555, $V = 14.5$) showed slow drifts of a few hundredths of a magnitude during the two nights of observation from Wise Observatory. These light variations were subsequently confirmed with the SARA data; the star was not present on any of the other observatories' frames. We note that it has a close companion which might affect the photometry, but this is unlikely owing to the applied MOMF photometry algorithm and because the magnitude changes were not correlated with seeing variations. The light variations of GSC 6589-0555 are rather complicated with a time-scale of about 20 h; no satisfactory multifrequency solution could be found.

To pinpoint the nature of these two variables, classification spectra were taken at the 1.9-m telescope of SAAO. Star A is of mid-to-late K spectral type. This spectral classification is corroborated by CCD colour photometry obtained at the SAAO

Table 1. Observing log of the 17th run of the Delta Scuti Network

Telescope	Instrument	Observer(s)	Hours of measurement
McDonald 0.9-m	PMT2	G. Handler, J. A. Guzik, T. E. Beach	104.7
McDonald 2.1-m	PMT2	G. Handler	54.0
ESO 0.9-m Dutch	CCD	T. Arentoft, C. Sterken	102.2
SAAO 0.75-m	PMT1	P. Martinez, F. Podmore, A. Habanyama, P. Meintjes, J. Brink	70.5
Siding Spring 0.6-m	PMT1	R. R. Shobbrook	40.9
Siding Spring 1.0-m	PMT1	R. R. Shobbrook	20.1
Perth 0.6-m	PMT1	P. V. Birch, P. Crake, G. Lowe, T. Smith	57.2
SARA 0.9-m	CCD	M. A. Wood, T. Oswalt, C. F. Claver	54.9
SAAO 1.0-m	CCD	L. A. Crause, D. W. Kurtz	22.1
Wise 1.0-m	CCD	E. M. Leibowitz, P. A. Ibbetson	10.4
SAAO 1.0-m	PMT1	R. Medupe	9.6
Kavalur 1.0-m	PMT3	B. N. Ashoka, N. E. Raj	3.2
Itajuba 0.6-m	CCD	J. E. S. Costa	0
Total			549.8

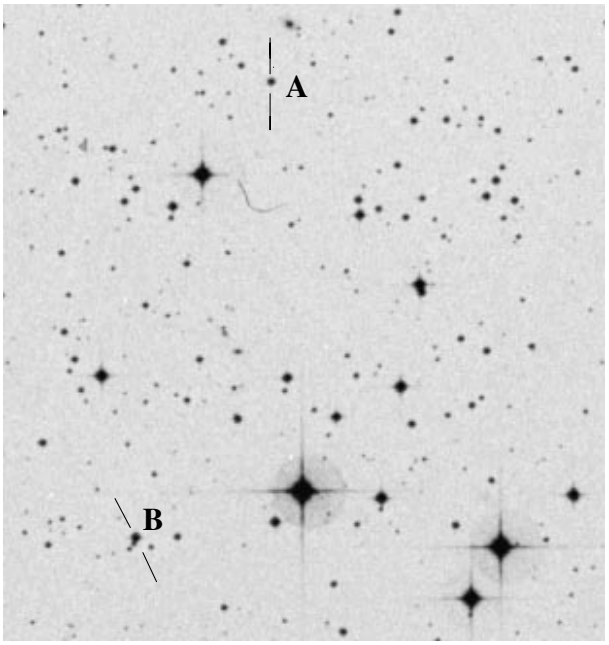

Figure 1. Finding chart for the new variables in the field of XX Pyx. Coordinates (Epoch 2000.0) are: Star A: α: $08^h58^m34\overset{s}{.}2$, δ: $-24^h33^m52^s$; Star B: α: $08^h58^m43\overset{s}{.}7$, δ: $-24^h40^m28^s$. The coordinates for star B are from the Guide Star Catalogue and should therefore be accurate, whereas the coordinates of star A were only roughly determined by us. North is on top and east to the left, the field of view is approximately 8×8 arcmin^2.

1.0-m telescope, which yielded $V = 15.12 \pm 0.02$, $(B - V) = 1.31 \pm 0.02$, $(V - R_c) = 0.72 \pm 0.04$, and $(V - I_c) = 1.40 \pm 0.05$. In accordance with the observed variability we think this is most likely a spotted star. Star B has a spectral type of late A/early F. It is therefore probably a variable star of the γ Doradus type. Needless to say, neither object was used as a comparison for XX Pyx.

3.2 Initial PMT reductions; constancy of the comparison star

The photoelectric measurements were reduced in a very similar way to that described by HPO (differences will be stated in what follows), i.e. we made use of the time-series of SAO 176755 to compensate for transparency variations or thin clouds (the latter naturally only in the case of multichannel observations) whenever necessary. This, of course, requires that this star be constant within the detection limit of oscillations of XX Pyx.

Non-variability of SAO 176755 had already been demonstrated for the new WET observations presented by HPO. However, the present study is based on a considerably larger amount of data. Therefore the expected noise level is much lower than previously, and the constancy of SAO 176755 has to be evaluated again. Another reason for doing so is that some variable stars can change their amplitude of variability with time; as a result some stars may appear constant at certain times, but variable at others.

We first considered the CCD photometry. Usable measurements of SAO 176755 were obtained during the first 11 nights (50.4 h) of SARA observation. On all the other frames the fields were either too small to acquire the star or its images were partly saturated (for obvious reasons the integration times were optimized for XX Pyx and not for one of its potential comparison stars). We computed an amplitude spectrum of these reduced data and found

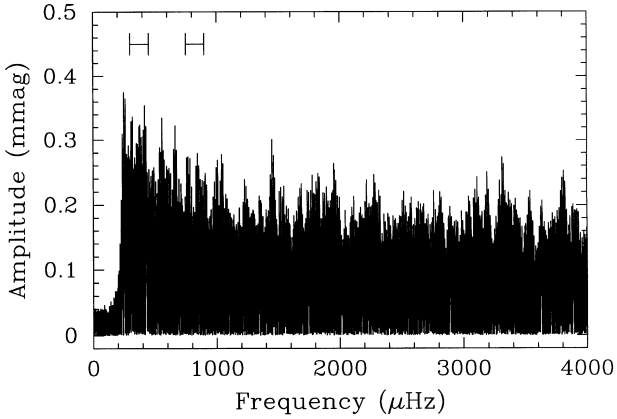

Figure 2. Amplitude spectrum of the time series of the comparison star SAO 176755 out to the Nyquist frequency. No variability with an amplitude larger than 0.4 mmag can be discerned; the distribution of the peaks is compatible with noise. The sharp decrease in amplitude at frequencies below $\approx$200 μHz is due to low-frequency filtering. The frequency ranges of interest for XX Pyx are indicated.

no variations with an amplitude larger than 1 mmag. Despite our attempts to suppress image motion on the frames, we found a clear $1/f$ component in the amplitude spectrum. As this is also true for the other comparison stars, we do not consider it to be intrinsic to SAO 176755.

Our next step was to select the photoelectric multichannel data which were taken under photometric conditions (25 nights from McDonald Observatory) and to reduce the comparison star data. We subtracted a polynomial or spline fit to the sky background, removed bad points and corrected for extinction. We also performed some low-frequency filtering of the data (as we will do later for the programme star observations as well; we will discuss this procedure further below) as we wanted to eliminate possible PMT drifts and because we were only interested in variability occurring on the same time-scale as the target star's pulsations. We then filtered out the slow variations in the CCD time-series, multiplied the resulting magnitudes by 1.32 (the average theoretical B/V amplitude ratio for δ Scuti-type pulsations following Watson 1988), and merged it with the photoelectric light curves after converting the times of measurement into Heliocentric Julian Date (HJD). Then we calculated the amplitude spectrum of the combined time-series comprising 143.1 h of measurement, which is shown in Fig. 2.

There is no evidence for variability of SAO 176755 in Fig. 2 within the accuracy of our observations. We therefore conclude that it can be used safely to correct the programme star time-series if taken under non-perfect photometric conditions. Thus we were able to proceed to the reduction of the variable star time series obtained with PMTs. As before, we first corrected for sky background, bad points and extinction. Whenever necessary, a differential time series relative to SAO 176755 was constructed. For multichannel photometers, this was done on a point-by-point basis. However, boxcar smoothing of the Channel 2 data was applied whenever possible so that as little additional noise as possible was introduced in the light curves of XX Pyx; the width of the smoothing function was chosen depending on the time-scale on which transparency variations occurred. In the case of single-channel photoelectric observations, low-order polynomials or splines were fitted through the comparison star measurements and the fits were subtracted from the target star observations.

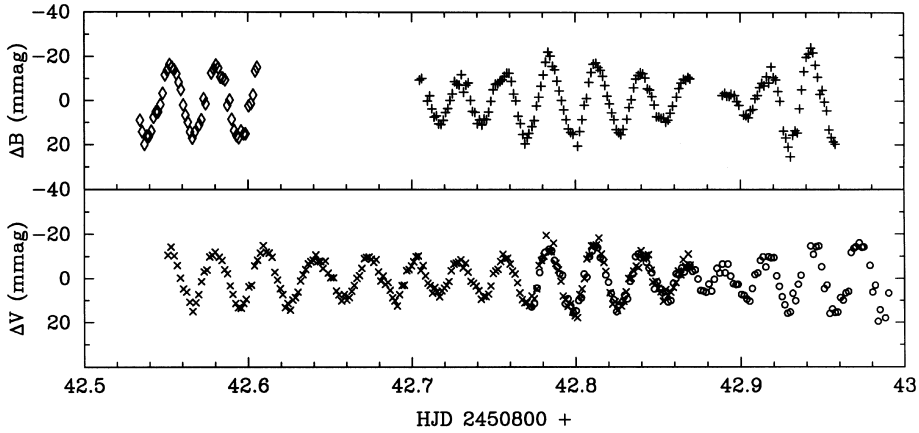

Figure 3. Some light curves obtained during the campaign. Diamonds: photoelectric SAAO data, plus signs: photoelectric McDonald observations, crosses: CCD measurements from ESO, open circles: SARA CCD light curve

3.3 Final reductions; low-frequency filtering

Because our primary goal is to detect as many pulsation frequencies of XX Pyx as possible, we are interested in obtaining the lowest possible noise level in the frequency range of interest. However, low-frequency noise generated for example by residual sky transparency variations, tube drift or image motion on the CCD detector can increase the noise at higher frequencies due to spectral leakage. Therefore, we decided to subject our time series to low-frequency filtering. We are aware that this destroys possible long-period stellar signals, but our combined data set is so inhomogeneous that such signals are hardly to be trusted. This had actually been a severe problem in the analysis of the first multisite data on the star (Handler 1994). We must further note that low-frequency filtering can be a dangerous procedure and has therefore to be applied with great care. By no means do we want to compromise the information supplied by the intrinsic variability of the star.

We proceeded as follows: we calculated the HJD for the preliminarily reduced light curves and combined the data for the different filters. Then we performed a frequency analysis of these data sets and removed a synthetic light curve consisting of all the detected signals due to pulsation from the time-series. This gave us a good indication of the frequency range excited in the star; we found that pulsational variability of XX Pyx only occurs at frequencies larger than 300 μHz. Based on this result we decided to filter out variations with frequencies less than 230 μHz ($20\,d^{-1}$).

To accomplish this, we split the original and residual light curves into those of the individual runs. We visually inspected them and we calculated amplitude spectra of all these different residual time series. Then we calculated synthetic light curve fits to the residual data, by fitting straight lines and/or sinusoids with all detected frequencies below 230 μHz to these residuals and we subtracted these synthesized low-frequency signals from the corresponding original light curves.

As the last step, we summed the final PMT and CCD light curves into 120-s bins to give all the observations equal weight and to decrease the number of data points to a reasonable amount. This time-series will be frequency-analysed in the next section.

We show some examples of our reduced light curves in Fig. 3. These were obtained during the part of the campaign with the highest duty cycle of the observations, but they are typical concerning data quality; they are not our best light curves. We refrain from showing all our data, as this would fill five journal pages at a reasonable scale. We will do that, however, in a publication to be submitted to the Journal of Astronomical Data, where we will also make our reduced data (9139 *B* and 5415 *V* measurements after binning) publicly available.

4 FREQUENCY ANALYSIS

4.1 Linear frequency analysis

Our frequency analysis was performed with an updated version of the program PERIOD (Breger 1990). This package applies single-frequency Fourier analysis and simultaneous multifrequency sine-wave fitting. We extended it to be able to handle large data sets with a rich frequency content.

We calculated the spectral window and amplitude spectra of our data as well as amplitude spectra of residual light curves where the previously identified periodicities were removed by means of a fit consisting of simultaneously optimized frequencies, amplitudes and phases. The frequencies were derived from the *B* filter data (which have a better spectral window and span a larger time base) and were kept fixed for the *V* filter observations to minimize effects on the amplitudes and phases due to mutual influence of the different signals.

All the parameters of our multifrequency fits are here assumed to be constant over the duration of the data set. Therefore we call this part of our frequency analysis *linear*. Results for the different filters are plotted in Fig. 4.

After the detection of 13 frequencies we decided to combine the residual *B* and *V* light curves; aliasing in the *V* filter data does not allow a convincing representation of the results in this filter after that point. We made use of these 13 frequencies to determine a scale factor required to merge the *B* and *V* residuals. It must be pointed out that different pulsation modes ought to have different amplitude ratios in the two filters; this is a known tool for mode discrimination. Therefore one should only merge such data as late as possible during a frequency analysis, i.e. the error of the determination of the amplitude ratio must considerably exceed its intrinsic scatter to avoid the introduction of artefacts.

Consequently, we determined the amplitude ratios for all the 13 modes and we adopted the median of these ratios (which amounted to 1.29) as the multiplication factor for the *V* filter

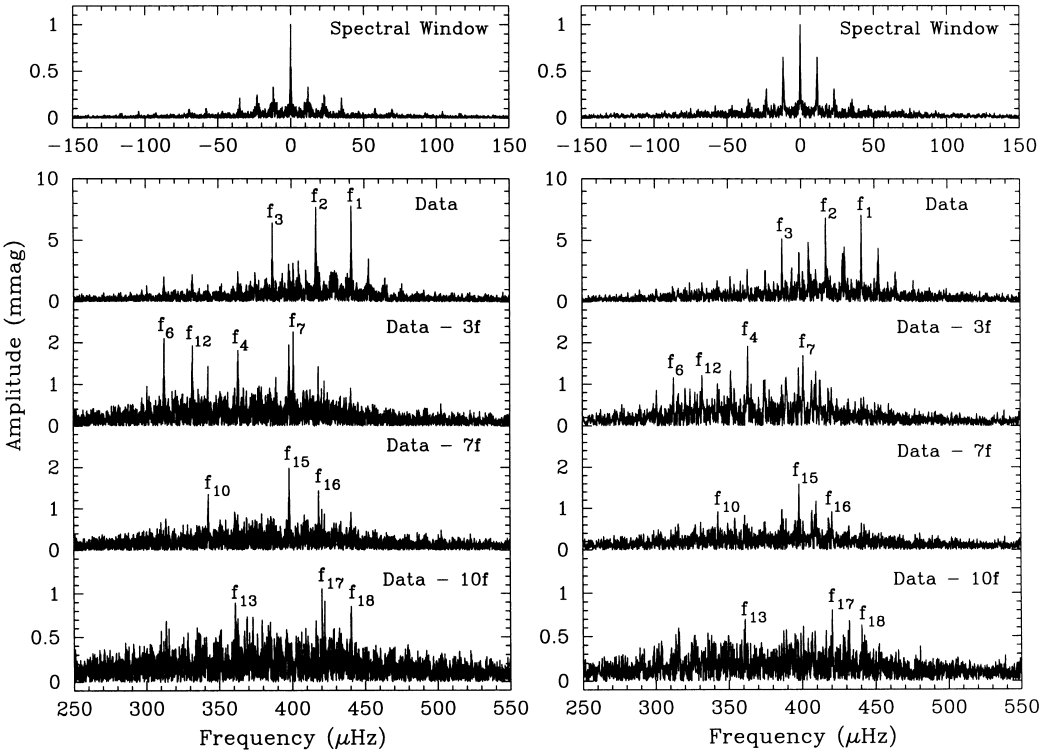

Figure 4. Spectral window and amplitude spectra of our *B* (left-hand side) and *V* (right-hand side) light curves and the results of removing three, seven and ten simultaneously optimized frequencies. The signals taken out from one panel to the next are labeled; the numbering is consistent with that used by HPO. Frequencies already known are f_1–f_{14}, all peaks with higher indices correspond to new modes which are now at higher amplitude due to the star's well-known amplitude variations. For reasons of presentation we stop this analysis after the detection of 13 frequencies.

residual light curves. We prefer the median over the mean to minimize the effects of 'outliers'. We then searched the combined data for further periodicities and display the result in Fig. 5. The frequencies derived at this step were determined from optimizing the fit for the combined residual data set, but they were kept fixed for the following determination of the amplitudes in the different filters for the same reason as explained before.

We need to clarify the steps of the frequency analysis presented in Fig. 5. In the combined residual data set (after removal of the contribution of 13 periodicities) we first tried to identify frequencies which were already detected by HPO, but not yet found in the present data set. These frequencies are labeled with arrows together with their identification in the upper half of the second panel of Fig. 5. All of them are present, however with small amplitude.

In the lower half of the second panel of Fig. 5 we show the residual amplitude spectrum after removing 17 periodicities. We can detect two more pulsation frequencies (again denoted with arrows and their identifications), and we indicate two further peaks with arrows close to them.

These two peaks and the peak labelled f_{18} in Fig. 4 have something in common: they are very close (within 0.5 μHz) to the pulsation frequencies f_1, f_2 and f_4. They are, however, fully resolved. The two unlabelled arrows in Fig. 5 actually denote the exact frequencies of f_2 and f_4. These close peaks are reason for concern as will be explained below; we stop the search for pulsation frequencies by means of linear frequency analysis at this point. We just add that the highest peaks believed to be noise in this frequency range have an amplitude of about 0.5 mmag.

However, we can still search for the presence of combination frequencies in our data.[1] Some have already been detected by Handler et al. (1996), but only one 2*f*-harmonic was significant. Because of our large new data set we can hope to increase the number of confirmed combination frequencies. Of course, the data reduction techniques applied only allow us to look for frequency sums; the frequency differences lie in the low-frequency range where we have previously filtered the data.

The lowest panel of Fig. 5 presents the frequency spectrum of XX Pyx in the range where combination frequencies are to be expected. In the upper half of this panel three peaks stand out; they all correspond to combination frequencies. After including the signals due to these frequencies in the light curve solution, the three next highest peaks can also be identified with combination frequencies (lower half of the lowest panel of Fig. 5). We note that a residual amplitude spectrum after adopting these three further signals exhibits more peaks whose frequencies coincide with combinations of pulsation frequencies but their amplitudes are comparable to those of the highest noise peaks (≈0.18 mmag) in the corresponding frequency domain. We therefore refrain from taking them into account.

At this point we find it useful to summarize our preliminary results from the linear frequency analysis and we do so in Table 2. To give an impression of the accuracy of these values, we also quote formal linear least-squares error sizes on our frequencies and amplitudes using the formulae of Montgomery & O'Donoghue (1999). These error bars should only be taken as a rough guide and are certainly underestimates, as will become clear in Section 4.3.

[1] This will provide us with an important clue used in the following analysis and in the interpretation of our results.

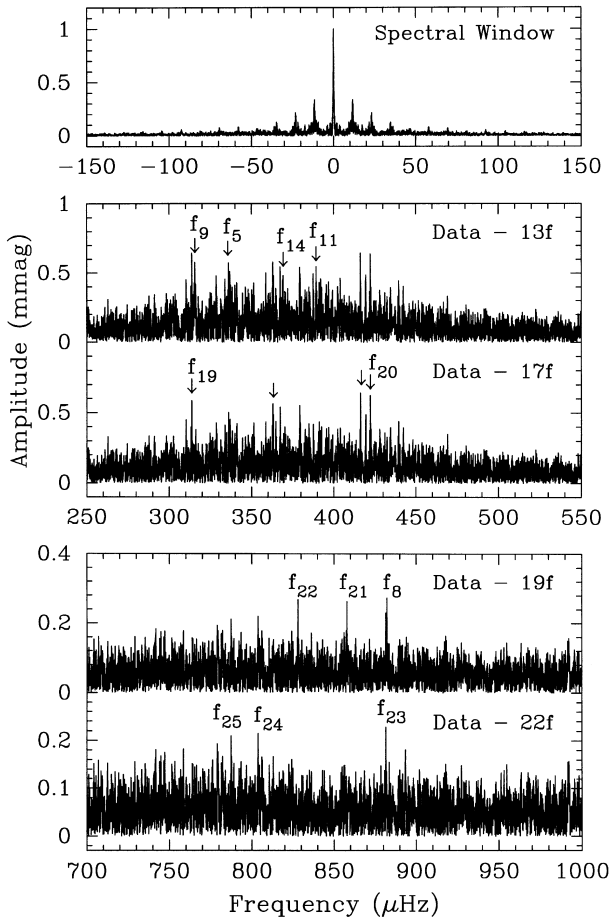

Figure 5. Spectral window and amplitude spectra of our combined *B* and *V* data for both pulsation as well as combination frequencies. The train of thought in this part of the analysis and the meaning of the indicated peaks are explained in the text.

4.2 Why go non-linear?

The main goal of our frequency analysis is to detect as many intrinsic pulsation frequencies of XX Pyx as possible. However, based on a simple numerical simulation we suspect that we have not yet exploited the full frequency content of our data: we calculated amplitude spectra of data consisting of white noise only, with the same standard deviation, number of data points and time distribution as the real data and 'reduced' them in the same way as the original measurements; the resulting noise level was about a third of that of the observations, suggesting that further signals could be present in the data.

As has been pointed out in the Introduction, XX Pyx is known to exhibit detectable amplitude variations on time-scales as short as a month (HPZ). Our data set spans almost three months. Therefore it can be suspected that these peaks close to several of the stronger modes could be caused by intrinsic amplitude (and possibly frequency) variations during the observations.[2] Preliminary tests showed that this is indeed the case and we must conclude

[2] Another reason for the appearance of such close peaks would be mismatches in the filter passbands between the different observatories, generating apparent amplitude modulations. Estimates of the size of such effects (Handler 1998) showed however that they would not be noticeable in the amplitude spectra.

Table 2. Results of the linear multifrequency solution for XX Pyx derived from the Delta Scuti Network measurements acquired in 1998. Formal frequency error estimates range from ±0.0004 μHz for the strongest modes to ±0.02 μHz for the weakest combination frequencies; the formal errors in amplitude are ±0.055 mmag for *B* and ±0.054 mmag for *V*.

ID	Freq. (μHz)	Freq. (d^{-1})	*B* ampl. (mmag)	*V* ampl. (mmag)
f_1	441.085	38.1098	7.80	6.53
f_2	416.813	36.0126	7.69	6.49
f_3	387.009	33.4376	5.88	4.56
f_4	363.424	31.3998	1.94	1.99
f_5	335.621	28.9977	0.27	0.45
f_6	312.624	27.0107	2.08	1.22
f_7	401.188	34.6626	2.43	1.99
$f_8 = 2f_1$	882.171	76.2196	0.30	0.20
f_9	315.494	27.2587	0.55	0.35
f_{10}	342.779	29.6161	1.53	1.00
f_{11}	389.271	33.6330	0.44	0.49
f_{12}	332.178	28.7002	2.06	1.32
f_{13}	361.143	31.2028	0.91	0.72
f_{14}	369.207	31.8995	0.64	0.17
f_{15}	398.166	34.4016	2.15	1.83
f_{16}	418.248	36.1366	1.54	0.75
f_{17}	420.446	36.3265	1.15	0.77
f_{18}	440.571	38.0653	1.01	0.72
f_{19}	313.678	27.1018	0.58	0.51
f_{20}	422.322	36.4887	0.77	0.35
$f_{21} = f_1 + f_2$	857.898	74.1224	0.26	0.22
$f_{22} = f_1 + f_3$	828.095	71.5474	0.26	0.20
$f_{23} = f_1 + f_{18}$	881.656	76.1751	0.21	0.23
$f_{24} = f_2 + f_3$	803.822	69.4502	0.20	0.18
$f_{25} = f_{11} + f_{15}$ or $f_{14} + f_{16}$	787.437	68.0345	0.22	0.18

that classical frequency analysis methods such as applied in Section 4.1 are not adequate for the present data set. To reach our goal of detecting the maximum number of intrinsic pulsation frequencies and to examine the suspected amplitude and/or frequency variations during the observations, the latter have to be quantified; we need to perform a *non-linear frequency analysis*.

Before starting with this procedure, we turn to the discussion of those close peaks appearing in the vicinity of the pulsation frequencies f_1, f_2 and f_4. We have labelled one of them as f_{18} and included it in our linear frequency solution, but we have not yet explained why.

We have reason to believe that this is an independent pulsation mode. f_{18} is very close to the mode f_1; the latter is the only independent pulsation mode for which a 2*f* harmonic is reliably detected (we called it f_8). This harmonic is just the mathematical result of the non-sinusoidal pulse shape of f_1. Yet we also found a peak very close to this harmonic – f_{23} – which is the sum frequency of f_1 and f_{18} (see Table 2). If f_{18} were an artefact which describes an amplitude and/or frequency variation of f_1, the harmonic of f_1 would be modulated in exactly the same way; therefore the presence of f_{23} would be expected. However, in this case the amplitude *ratio* of f_1/f_{18} and f_8/f_{23} must then be the same. These amplitude ratios and their error sizes amount to 7.72 ± 0.39 for f_1/f_{18} and 1.36 ± 0.38 for f_8/f_{23} and are therefore significantly different from each other. We note, however, that this argument is only valid under the assumption that the pulse shape of f_1 does not vary when this mode changes its amplitude. HPZ have shown that this assumption is justified.

Regrettably, we cannot use similar arguments for all the other peaks appearing close to those corresponding to the dominating pulsation modes, because f_1 is the only mode with a detectable

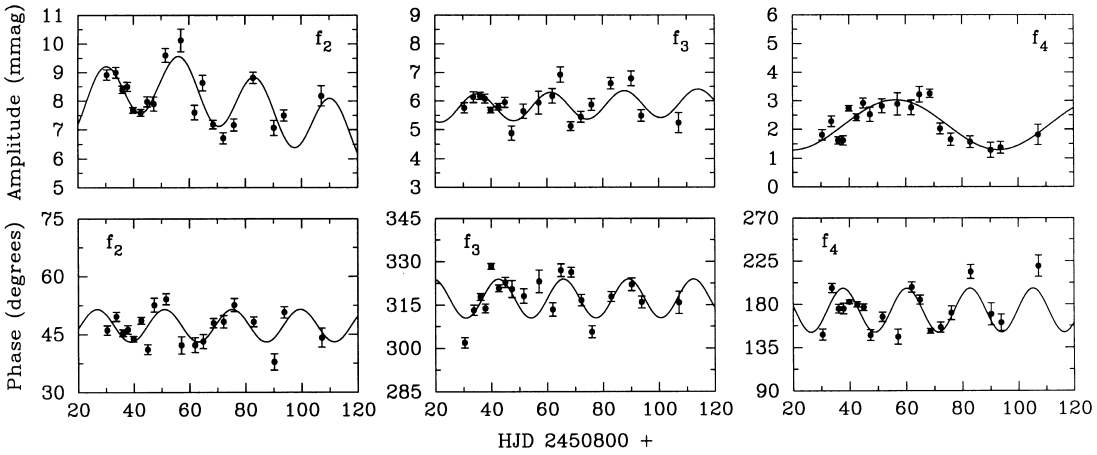

Figure 6. Amplitude and frequency variations of the three most unsteady modes. The adopted fit to compensate for them is superposed.

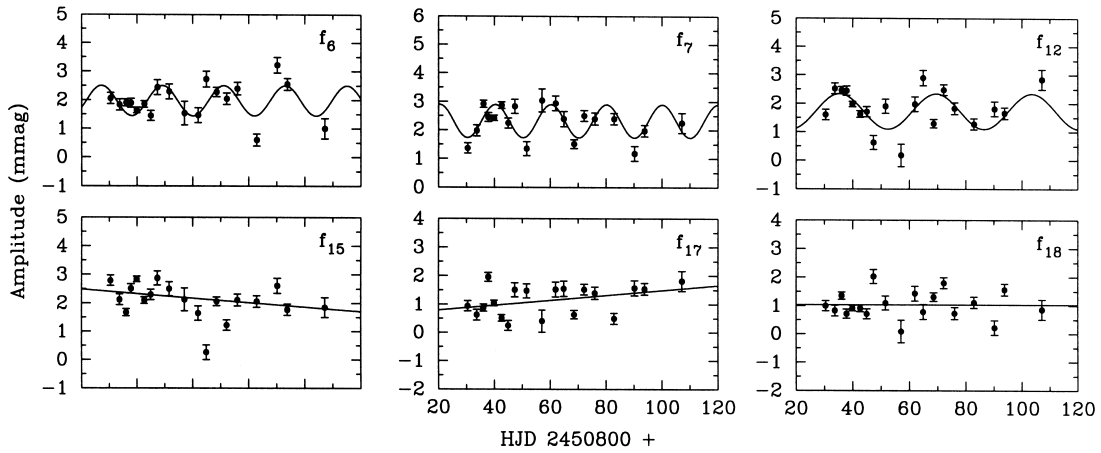

Figure 7. Temporal behaviour of all the other modes which were classified as having variable amplitudes. For comparison, the result for one mode with constant amplitude (f_{18}) is also displayed; the correspondingly adopted fits are shown as well.

harmonic. To be conservative, we will therefore not consider these close peaks to be caused by possible pulsation modes.

Having set the stage this way, we can now start with our non-linear frequency analysis. This is of course a very delicate procedure and has, to our knowledge, never been attempted before in a similar way. Consequently, we will proceed as carefully as possible, describing our analysis as comprehensively as possible. We will also provide discussions or justifications of our decisions whenever deemed necessary.

4.3 Non-linear frequency analysis

To start our analysis, we first needed to isolate the light variations of the mode whose amplitude and/or phase variations were to be characterized. Therefore, we fitted the complete linear frequency solution to all the data, determined all the frequencies, amplitudes and phases and stored them. For each frequency under consideration, we then calculated a synthetic light curve from this solution, leaving out the parameters of the signal in question. This serves to minimize the effects of mutual influence of the frequencies as opposed to calculating an optimized $(n-1)$-frequency fit to the data. Our fit was subtracted from the data, leaving them with only the light variation due to this single mode plus noise (plus possible further periodic signals). This was done for all the 19 pulsation modes detected so far and we will call the resulting data sets 'single-mode data sets' in what follows.

We note that this fit was calculated for the combined B plus scaled V data set (again a median amplitude ratio of 1.29 was adopted). In this way we gained a better time-distribution of the data at the expense of increasing the uncertainty in amplitude determination; the latter is easier to take into account and we will attempt to do so later.

We then had to split the data sets into suitable subsets for examining amplitude and phase stability. The optimal solution would be to have as many subsets as possible, and all of these should have good spectral window functions in order to suppress the influence of other modes on the one under scrutiny. With real data this cannot always be achieved. Consequently, we attempted to partition the data as optimally as possible; for sections of data where we could not obtain a very clean spectral window we increased the time-base. We ended up with 19 non-overlapping subsets of data containing between 367 and 1152 points and spanning between 1.28 and 4.85 d. In other words, we had at least 13 cycles of any mode in each subset of data available.

Continuing the analysis, we took all the single-mode data sets, fitted the corresponding frequencies again and optimized them. Then we fixed the frequency and determined the corresponding amplitude and phase, as well as the error estimates for those quantities (following Montgomery & O'Donoghue 1999; actual

values will be shown in Figs. 6 and 7), in all the 19 subsets. The temporal behaviour of the amplitudes and phases of the different modes was investigated for variability.

We noticed that several modes seemed to show amplitude and phase variations, which prompted us to seek criteria to distinguish modes which were variable in time. However, this could not be done in a generally applicable way. First of all, we noticed that our errors were not random. Comparing the rms scatter of the amplitudes and phases determined for all the modes in all the subsets with the mean of the standard errors we derived before, we found that the real scatter was a factor of 2 or more higher than the mean of the formal error estimates.[3] The latter has also been recognized by Koen (1999) in his analysis of high-speed photometry.

Furthermore, the behaviour of the amplitudes in time was quite different from mode to mode: some seemed to be linearly increasing or decreasing, some exhibited apparent cyclical variations, and some showed combinations of the features described above. Finally, the error in phase does, of course, depend on the amplitude itself. Because of all this, distinguishing between variability and constancy is not straightforward; we decided to rely upon common sense and experience. In other words: our results will reflect personal bias.

After having classified the amplitude or phase behaviour of the modes initially as:

(i) variable in amplitude and phase;
(ii) variable in amplitude only;
(iii) constant;

we modified the fitting procedure. We first note that we did not find a mode which was variable in phase only, but this could be serendipity. Another result of this first examination was that allowing for phase variability of low-amplitude (<1.5 mmag) modes is not useful; the phases of such modes are too weakly constrained. Therefore any apparent variability is doubtful.

The modification of the fitting procedure consisted of leaving phase as a free parameter only for those modes where definite phase variations were detected. For all the other modes we fixed the phase and, if the mode was found to be constant in amplitude as well, also the amplitude. This decreases the number of free parameters in the fitting procedure and was intended to avoid generating artefacts. For example, the calculated amplitudes of weak modes tend to become systematically too large when allowing their phases to be free parameters, exposing the analysis to the danger of overcompensating for their contributions.

The resulting diagrams of amplitude and phase versus time were then fitted according to which kind of variability these parameters exhibited. Besides the diverse behaviour of the amplitudes described above, cyclical phase variations were also detected for some of the stronger modes. Consequently, we constructed synthetic light curves for all the different modes according to their behaviour, i.e. we generated sinusoids whose amplitudes and phases varied in time correspondingly.

[3]This is probably partly due to mutual influence of the different modes; we performed simulations by generating multiperiodic synthetic light curves sampled the same way as the observations, using the frequencies from the linear solution, constant amplitudes and phases of the component signals, convolved with Gaussian noise and analysing them just as the real data. We found some small systematic trends in the reconstructed amplitude and phase behaviour over time. Another source of systematic error would be the presence of further pulsation modes or of residual transparency variations in our data. To examine the contribution of the latter, we compared the rms scatter of amplitude determinations of subsets of our comparison star data with the mean of the formal errors thereof. We found that the 'real' errors were about 50 per cent larger than the formal values. All these effects together can therefore explain at least a large fraction of the discrepancy between the observed and formal errors.

Table 3. Amplitude and phase variations of some pulsation modes of XX Pyx during the 1998 observations; in case of cyclical variability an approximate time scale is given. Only variable modes are listed.

ID	Amplitude variability	Phase variability
f_2	Linear and cyclical (25 d)	Cyclical (25 d)
f_3	Cyclical (25 d)	Cyclical (25 d)
f_4	Cyclical (70 d)	Cyclical (25 d)
f_6	Cyclical (22 d)	–
f_7	Cyclical (20 d)	–
f_{12}	Cyclical (35 d)	–
f_{15}	Linear	–
f_{17}	Linear	–

This is, of course, not yet the best solution. We already mentioned the potential danger of mutual influence of the pulsation modes. Hence we decided to apply our non-linear frequency analysis iteratively. Therefore, we again calculated synthetic light curves, including the preliminary results from the nonlinear frequency analysis for the construction of the single-mode data sets. We then repeated the procedure of searching for and classifying the temporal variability, fitting these data with as few free parameters as possible and finally constructing synthetic light curves for the individual modes. After this iteration, the scatter in the amplitudes and phases for the different subsets of data decreased, indicating convergence and thereby justifying the iteration.

At this point we can finally display the results of our analysis. Our final classifications of the amplitude and phase variability of the modes are summarized in Table 3; the determined amplitude and phase variations are displayed in Figs 6 and 7. We point out that the terms we use to describe the amplitude and frequency variations correspond to the functions we fitted to compensate for them; their intrinsic shape might well be different. We stress again that our main aim in constructing the fits was to suppress spurious peaks in the amplitude spectrum due to the temporal variability of some modes. We seek no physical justification for the types of the fits; some might be more suggestive, some less.

Still, we found it useful to derive some formal assessment for our choices of the fits. We evaluated our solutions by means of the Bayes Information Criterion (BIC)

$$\mathrm{BIC} = \frac{p \log N}{N} + \log s^2,$$

where p is the number of free parameters of a model fitted to data, N the number of data points and s the standard deviation of the residuals. The BIC means that for every free parameter introduced into the fitted model the standard deviation of the residuals should be decreased by a certain amount; the goal of testing models with the BIC is to minimize the latter. In the present case ($N = 19$) the rms residuals must decrease by 8 per cent for each new free parameter to be accepted.

We tested several models with the BIC for each mode: constant amplitude/phase ($p = 1$), linearly changing amplitude ($p = 2$; a

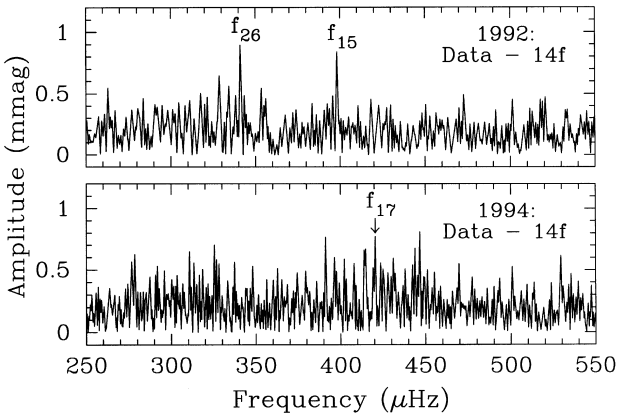

Figure 8. Amplitude spectra of the residuals of the 1992 and 1994 WET observations after prewhitening the frequency solution determined by HPO. In the 1992 data, the new mode f_{15} found in this study is present, and a completely new mode (f_{26}) is also revealed. In the 1994 data, our new mode f_{17} can be detected. No other new modes could be found in these smaller data sets.

linearly changing phase would of course mean the chosen frequency is incorrect) and sinusoidal amplitude/phase modulation ($p = 4$). The results of these tests supported our selections of the employed fits in every case; we were actually more conservative than the BIC would be. We note that the amplitude variations of f_2 were fitted with a higher-order model (sinusoid plus two straight lines, $p = 6$). The BIC also confirmed this choice.

Having quantified the amplitude and phase variations of the modes this way, we can now apply our non-linear multifrequency fit to the data. However, this again requires caution. The scale factor we applied to the *V* filter data is, as mentioned previously, not expected to be the same for all the modes. In addition to the dependence of the amplitude ratio on the type of the pulsation mode, the amplitude variations also have an effect, as our *B* and *V* filter data are mostly not simultaneous and therefore sample different phases of the amplitude variations of different modes. Before our nonlinear frequency analysis this was an unknown factor and could not possibly have been taken into account; at this point it can (at least to first order). On the other hand, deviations of the originally adopted scale factor from its 'real' value would only generate noticeable results for the three strongest modes: our previous detection level was around 0.5 mmag. Therefore, even a large difference (say, 10 per cent) from the real amplitude ratio would only generate noise peaks much smaller than this detection level for the weaker modes.

Consequently, we split the full non-linear synthetic light curve into two subsets corresponding to the original *B* and *V* data. Then we performed a linear frequency analysis on these data as described in Section 4.1, adopting the exact frequencies determined there. We stopped at the point where the *B* and *V* residuals were originally merged. Then we compared the amplitude ratios between the results in Table 2 and those for the non-linear solution in each filter for each mode and determined scale factors for each of the three strongest modes separately. These were applied to the fits for the corresponding mode, and the resulting synthetic light curves were added together and adopted as our final non-linear multifrequency fits. These were subtracted from the observed light curves in each filter. The residuals were again combined with a scale factor of 1.29 for the *V* filter data and subjected to additional linear frequency analysis. Before presenting these results, we will however reconsider the published observations of XX Pyx.

4.4 Reanalysis of the 1992 and 1994 data

As already mentioned in the Introduction, amplitude variations of pulsating stars can serve to detect more modes over time than would be possible with one data set obtained in a short period of time only. XX Pyx was initially observed during two WET runs. The analysis of these observations (HPO) resulted in 13 pulsation frequencies, but also suggested that more modes are likely to be excited in the star. Obviously, some of these suspected further modes might already have been detected in the present data set, and one can hope that by including the corresponding frequencies in a reanalysis of the older data, some more modes which have amplitudes too low to be detected in the new data can be revealed in the WET observations because of the consequently decreased noise level.

Therefore we re-reduced the WET observations in accordance with the procedure outlined in Section 3.3, subtracted the multifrequency solution by HPO from these data and searched the residual amplitude spectra for new modes. We display the result in Fig. 8.

Indeed, in the 1992 data, the new mode f_{15} clearly detected in this study is obviously present. After removing this signal from the data, a completely new mode f_{26} dominates the residual amplitude spectrum. This peak has already been discussed by HPO and it barely escaped detection then. Now we have no doubt it is intrinsic to XX Pyx as it is also present (but not detected) in the 1998 data. We note that the combination frequencies f_{21} and f_{22} are also present in this data set (see Handler et al. 1996 for a graphical representation) and can now be included as well.

The lower panel of Fig. 8 shows the residual amplitude spectrum of the WET measurements in 1994. Here we can only detect f_{17} in addition, but no further peaks can seriously be claimed as being due to pulsation modes in this data set alone. It should be noted that the 1994 WET data do not have a very good spectral window. Therefore some modes may have artificially decreased amplitudes there because of spectral leakage of prominent neighbours which were prewhitened. Finally, we would like to comment that the time bases of individual WET runs on XX Pyx are smaller than any time scale of amplitude or frequency variations we discovered in the new DSN data. Hence they should hardly affect the frequency analysis of the 1992 and 1994 measurements.

4.5 Frequency analysis of the combined residuals

As the last step of our frequency search, we put all the residual data together and we looked for possible further frequencies in the combined data set. Of course, it would perhaps be more correct to merge all the original data, then perform a frequency analysis on this data set with fixed-frequency solutions allowing for variable amplitudes and phases and to examine the resulting residuals. However, because of the nature of the amplitude and frequency variations already discovered and because of the large gaps in the combined data set, this would lead to severe complications in the analysis. In addition, we would need to combine the *B* and scaled *V* data beforehand, which have different amplitude ratios and which could also show phase shifts relative to each other. We are therefore afraid that such an approach would generate more

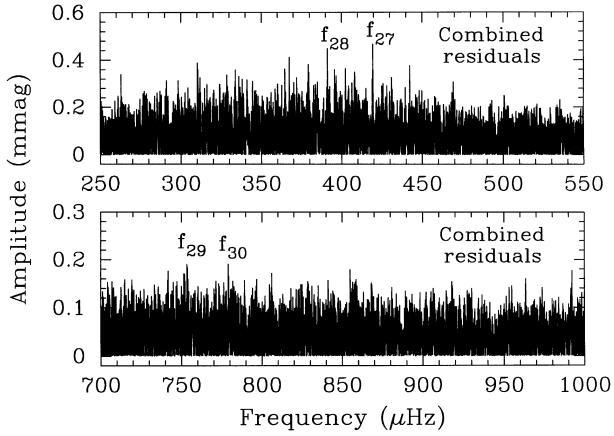

Figure 9. Upper panel: amplitude spectra of the residuals of all three multisite campaigns. Two further pulsation modes can be detected. Lower panel: two more combination frequencies manifest themselves.

artefacts than everything else and refrain from it. Instead, we just examine the combined residuals consisting of the data from each campaign pre-whitened separately. This could suppress possible intrinsic peaks, which can then not be detected, but it is definitely the safer modus operandi.

Fig. 9 shows the results of the analysis of the combined residuals. In its upper panel, the detection of two more frequencies of pulsation is presented. We note that peaks at these frequencies are present (often prominently) in the residuals of each of the 1992, 1994 and 1998 data sets. In the lower panel of Fig. 9, the two highest peaks in the domain of combination frequencies occur at sums of known mode frequencies; the frequency of peak f_{29} can be identified with $f_1 + f_6$, whereas f_{30} is consistent with three frequency combinations: $f_3 + f_{28}$ or $f_{13} + f_{16}$ or $2f_{11}$. We cannot judge which of the identifications is correct.

4.6 Frequency content of the light curves of XX Pyx and significance of mode detection

Until now, we did not attempt to prove that the frequencies claimed by us represent significant detections. This was intentional, because different modes were found in different data sets, for which different circumstances apply and separate discussions might hence have generated confusion. We now consider this altogether.

The most widespread (and in our view most useful) criterion to assess the significance of detections in frequency analyses was proposed by Breger et al. (1993), which adopts an amplitude signal-to-noise ratio of 4 as the limit for a reliable detection. We refer to the aforementioned paper and to Handler et al. (1996) for discussions of this criterion and for prescriptions for its use. Later, Breger et al. (1999) suggested that a somewhat lower signal-to-noise ratio of 3.5 would serve as a good gauge for the reality of combination peaks as these must occur at predictable frequencies. So far, these criteria have never led to spurious answers and we will therefore adopt them for our analysis as well.

We calculated the amplitudes of all the modes and combination signals for the data sets in which the detections were reported in this paper. Then we determined the noise level following Handler et al. (1996) and calculated the resulting signal-to-noise ratios for all the peaks. The outcome is summarized in Table 4.

As one can see from this table, all the new frequencies correspond to certain detections according to the criterion used, although we caution that the combination peak with $S/N = 3.5$ only reached this value after rounding.

Table 4. The frequency content of XX Pyx from the combined analysis of the 1992–1998 multisite observations. The quoted amplitudes and signal-to-noise ratios correspond to different data sets, namely those where the amplitudes of the modes were determined for the *S/N* calculation: 98B means the *B* amplitude of the 1998 data, 98C denotes amplitudes in the combined 1998 *B* and *V* data set, 92 labels the 1992 WET data (mode detection in hindsight) and 929498 is the data set consisting of the combined residuals of all the multisite observations. Entries in the columns for amplitude and *S/N* labelled with colons correspond to modes which are variable in amplitude. The modes f_5 and f_{14} are not significant here, but they were clear detections by HPO.

ID	Freq. (μHz)	Freq. (d^{-1})	Ampl. (mmag)	*S/N*	Data set
f_1	441.09	38.110	7.80	65.3	98B
f_2	416.81	36.013	7.7:	61:	98B
f_3	387.01	33.438	5.9:	46:	98B
f_4	363.42	31.400	1.9:	15:	98B
f_5	335.63	28.998	0.35	2.9	98C
f_6	312.63	27.011	2.1:	18:	98B
f_7	401.18	34.662	2.4:	19:	98B
f_8	882.16	76.219	0.27	4.9	98C
f_9	315.50	27.259	0.51	4.3	98C
f_{10}	342.78	29.616	1.53	12.2	98B
f_{11}	389.28	33.634	0.52	4.0	98C
f_{12}	332.18	28.700	2.1:	17:	98B
f_{13}	361.14	31.203	0.91	7.1	98B
f_{14}	369.21	31.900	0.45	3.3	98C
f_{15}	398.17	34.402	2.2:	17:	98B
f_{16}	418.25	36.137	1.54	12.4	98B
f_{17}	420.45	36.327	1.2:	10:	98B
f_{18}	440.57	38.065	1.01	8.7	98B
f_{19}	313.67	27.101	0.59	4.7	98C
f_{20}	422.32	36.489	0.63	5.1	98C
f_{21}	857.91	74.123	0.27	4.7	98C
f_{22}	828.12	71.549	0.26	4.4	98C
f_{23}	881.52	76.163	0.24	4.3	98C
f_{24}	803.83	69.451	0.21	3.6	98C
f_{25}	787.37	68.029	0.21	3.5	98C
f_{26}	341.07	29.468	0.87	4.1	92
f_{27}	419.50	36.245	0.47	4.5	929498
f_{28}	391.20	33.799	0.44	4.2	929498
f_{29}	753.32	65.087	0.19	3.7	929498
f_{30}	779.03	67.308	0.19	3.6	929498

We find it useful to comment on the problem of mode detection a little further. Because we are investigating a very large data set, one could suspect that noise peaks can rather easily exceed our adopted *S/N* threshold. Scargle (1982) inferred a so-called false alarm probability criterion on which the reliability of frequency detection can be judged. It has however been pointed out by various authors (e.g. Martinez 1989) that this criterion gives overoptimistic results. The results are also quite dependent on the time-distribution of the data (Horne & Baliunas 1986). Because of all this, a comparison using the formal methods developed in the original papers does not seem useful.

We decided to do the following: we considered a hypothetical signal which is present in the 1998 data set with a *S/N* of exactly 4.0. To derive the false alarm probability of such a detection, we generated 300 data sets consisting of our residual data, but shuffled in time (investigating the combined data set of all campaigns would require an impracticably large amount of

computing time), and performed frequency searches on them. About 1.5 million peaks in the amplitude spectra were considered and their *S/N* was calculated in exactly the same way as for our observations. We found 12 peaks that exceeded the empirical criterion of $S/N = 4.0$, corresponding to a false alarm probability of 8.0×10^{-6} for a peak with this *S/N*. A similar experiment by generating data sets of random noise with the same temporal distribution as our real data gave a similar result (false alarm probability 7.1×10^{-6} for $S/N = 4.0$). The residuals of the observations are of course not random, but we use a determination of the *local* noise in our calculations. We therefore take the effects of non-random noise into account in first order. In any case, we add that we do not use such formal criteria alone to judge the reliability of peaks in the amplitude spectra. Other tests, such as investigating subsets of data are always performed in addition.

Finally, we carried out some experiments to find other possible frequencies, for example by dividing the data into carefully chosen subsets, e.g. the data of highest quality. We also invoked some frequency analysis techniques which employ weighting (Arentoft et al. 1998) but in no case could we discover further credible pulsation frequencies. We note however that the residual light curves often show features which clearly indicate periodic variability with the time scale of the detected pulsations, but these do not seem to be coherent. Amplitude spectra of subsets of such residual data often show strong peaks, but they never quite reach $S/N = 4.0$, which can be taken as further support for the use of this criterion. This apparent incoherence could be intrinsic (short mode life-times, amplitude variations of yet undetected modes) or be a result of multiperiodicity.

5 MODE TYPING

5.1 Frequency spacing

HPO reported the discovery of a preferred separation within the frequencies of pulsation modes they revealed in the light curves of XX Pyx. These authors suggested this was due to the presence of modes with alternating even and odd values of the pulsational quantum number ℓ for the following reasons:

(i) The number and frequency distribution of the detected modes required that more than a one ℓ-family be present.

(ii) Pulsational models show such sets of modes should occur alternatively in the excited range of radial overtones.

(iii) The evolutionary state of XX Pyx is consistent with this hypothesis only.

(iv) The characteristic frequency spacing is too large to be interpreted in terms of rotational splitting.

Making use of this result, HPO could infer the frequency spacing due to consecutive radial overtones and hence derive the mean density of XX Pyx; the latter is possible because this characteristic spacing is simply a measure of the sound crossing time through the star. Because this preferred separation is not the asymptotic one, HPO had to invoke model calculations to determine the mean density of XX Pyx.

For obvious reasons it is very interesting to check whether this mean frequency spacing is still present as we have now almost twice as many modes available. Therefore, we repeated the analysis described by HPO and we display the result in Fig. 10, which contains the Fourier power spectrum of the frequency values with amplitudes normalized to unity.

Comparing our result to that of HPO, we find practically no difference. In fact, the characteristic frequency spacing became even more significant. We follow the method described by HPO to refine the mean frequency spacing of consecutive radial overtones of XX Pyx to $53.6 \pm 0.5\,\mu$Hz. With this value we can also refine the star's mean density to $\bar{\rho} = 0.241 \pm 0.008 \bar{\rho}_{\odot}$.

As mentioned in the Introduction, the discovery of more pulsation modes of XX Pyx should lead to obvious patterns within the frequency values of the modes. To examine this idea, we show a schematic frequency spectrum with all the pulsation modes in Fig. 11.

Our prediction turned out to be correct. The modes of XX Pyx are grouped within narrow frequency intervals with some gaps in between. This is a clear indication of the expected essentially pure p-mode spectrum split by rotation.

As a matter of fact, the appearance of this schematic frequency spectrum can be used to estimate the stellar rotational velocity. If one considers a series of model frequency spectra of δ Scuti stars in the evolutionary state of XX Pyx and studies the development of their patterns depending on rotational velocity, the following features become apparent: for a slowly rotating model, the multiplet patterns form non-overlapping close groups. The faster the model rotates, the more the multiplets begin to overlap in frequency; gaps between the groups disappear. In a certain range of rotational rates, the modes seem to form regular groupings again, but the different subgroups are mixed in ℓ. The reason for

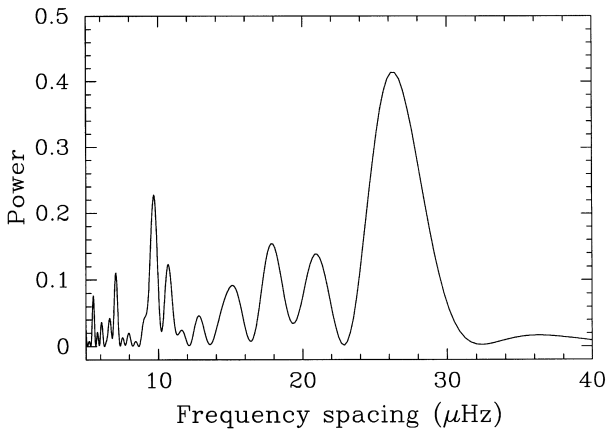

Figure 10. Search for a preferred frequency separation within the 22 detected pulsation modes of XX Pyx. This diagram is very similar to fig. 7 of HPO and therefore dramatically confirms their result for 13 frequencies.

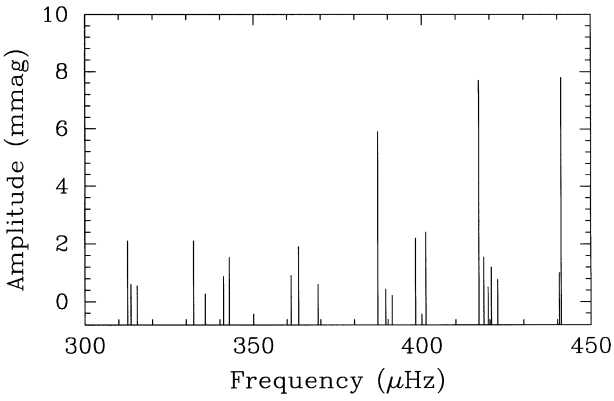

Figure 11. Schematic frequency spectrum of XX Pyx. Clear groupings of modes can be seen.

this 'clumping' of modes is that the second-order effects of rotation are of similar size as the first-order effects, causing the modes with $m \leq 0$ of the same k and ℓ to be very closely spaced in frequency, whereas the modes with $m > 0$ are mixed into the next groups of closely spaced modes at lower frequency. Increasing rotation even more, these groups again disappear, because the second-order effects begin to dominate. As we know that XX Pyx has a projected rotational velocity $v \sin i = 52 \pm 2\,\mathrm{km\,s^{-1}}$ (HPO), we can immediately rule out that the groupings seen in Fig. 11 consist of members of the same ℓ; rotational splitting would be too large even if $i \approx 90°$. Consequently, the rotational velocity of the star must be in the correct range for modes closely spaced in frequency, separated by gaps, to appear again. Hence we can predict that the rotation frequency of XX Pyx must be around $1.1\,\mathrm{d^{-1}}$ or its $v_{\mathrm{rot}} \approx 110 \pm 30\,\mathrm{km\,s^{-1}}$.

As pointed out by the referee, one would expect to see evidence for rotational splitting within the pulsation frequencies of XX Pyx. Considering the large number of theoretically expected modes we detected, the presence of several pairs of modes of $m = +1$ and $m = -1$ of the same k and ℓ is very likely. Such mode pairs should have very similar frequency differences ($\approx 2\nu_{\mathrm{rot}}$), as first-order rotational effects are small, second-order effects cancel for frequency differences of modes of the same $|m|$ and third- and higher-order effects are negligible. We actually performed a search for such frequency differences, but our results were inconclusive. The reason for this could either be unfavourable mode excitation or differential rotation.

Adopting the ranges of mean density and rotational frequency inferred above and assuming that most observed modes must be p-modes of radial order 4–6 (HPO) with $\ell \leq 2$, we attempted to perform an identification of all the modes by examining the mode patterns. Regrettably, our initial attempts failed, although parts of some solutions appeared quite promising. For example, the mode groups (f_9, f_{12}, f_5), (f_{14}, f_3, f_{11}) and (f_{17}, f_{18}, f_1) would be consistent with $\ell = 1$ triplets of $k = 4$, 5, 6 for a rotational frequency $\Omega = 0.9\,\mathrm{d^{-1}}$, but several of the remaining modes can then not be fitted reasonably with the remaining possibilities of $\ell = 0$ and 2. A definite mode identification therefore probably has to await detailed model calculations.

5.2 Phase shifts and amplitude ratios

To aid in identifying the excited modes with their pulsational quantum number ℓ, time-series colour photometry can be employed. Pulsation modes with different ℓ behave slightly differently when observed at different wavelengths, which can in principle be used as a mode discrimination tool (Balona & Stobie 1979; Watson 1988; Garrido, Garcia-Lobo & Rodriguez 1990; Balona & Evers 1999). The most widespread method utilizes amplitude ratios and phase shifts of the pulsations in two different filters for determining ℓ.

These values are in principle easy to determine from the observed light curves. However, as we have shown in Section 4.3, the amplitudes and frequencies of several modes are variable, which complicates the analysis. As a matter of fact, for these modes it only appears safe to use those parts of the data where simultaneous B and V filter photometry has been obtained to determine amplitude ratios and phase shifts: the intrinsic shape of the star's amplitude and frequency variations is not known. Thus, correcting for these to allow use of the whole data set is not justified. There are, however, only about 60 h of overlapping B and V measurements available.

Still, we calculated the amplitude ratios and phase shifts for each of the 11 strongest modes; the results are listed in Table 5. For modes which appear to be constant in amplitude and phase, the values in Table 5 were calculated from a linear multifrequency fit with fixed frequencies for the B and V data. For all the other modes, we examined the overlapping data pre-whitened by the other frequencies. These overlapping data were subdivided into parts which were significantly smaller than the time scales of the amplitude and frequency variations, and amplitude ratios and phase differences were calculated for each subset by fixing the frequencies. We adopted the mean value of the individual determinations as our result and the mean error of this mean for our error estimate. The error sizes for the modes constant in amplitude and phase in Table 5 are based on the formulae by Montgomery & O'Donoghue (1999), but the results were multiplied by a factor of two because of the correlated noise (see Section 4.3) to yield approximately realistic estimates.

As one can see from Table 5, the error estimates for the amplitude ratios and phase shifts for the modes f_1–f_3 are the lowest, which makes these modes the best candidates for a determination of ℓ. However, a comparison between the observed amplitude ratios and phase shifts for these modes and the theoretical 'areas of interest' (kindly calculated and provided by M.H. Montgomery) in an amplitude ratio/phase shift diagram for a

Table 5. Amplitude ratios and phase shifts for 11 modes of XX Pyx. See text for information on the determination of the quantities listed.

ID	Freq. (μHz)	A_B/A_V	$\phi_B - \phi_V$ (degrees)
f_1	441.09	1.194 ± 0.027	$+1.0 \pm 1.3$
f_2	416.81	1.245 ± 0.056	$+2.3 \pm 1.1$
f_3	387.01	1.272 ± 0.056	-2.3 ± 1.9
f_4	363.42	1.125 ± 0.016	-12.1 ± 7.7
f_6	312.63	1.449 ± 0.183	$+21.2 \pm 16.5$
f_7	401.18	1.204 ± 0.070	-3.6 ± 3.9
f_{10}	342.78	1.530 ± 0.207	-1.3 ± 7.8
f_{12}	332.18	1.758 ± 0.319	-1.0 ± 2.5
f_{15}	398.17	1.175 ± 0.196	$+8.5 \pm 6.2$
f_{17}	420.45	1.063 ± 0.306	$+31.2 \pm 16.4$
f_{18}	440.57	1.402 ± 0.272	$+1.0 \pm 11.1$

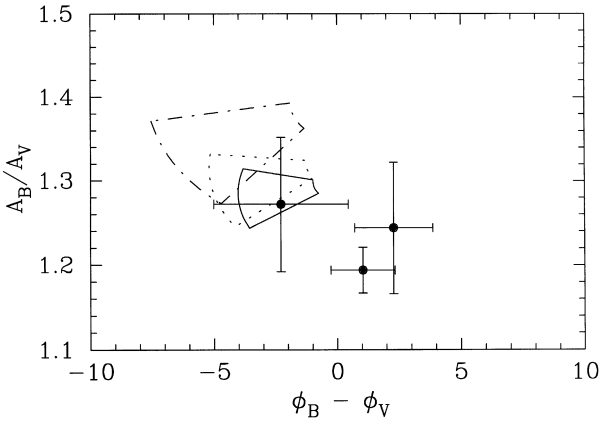

Figure 12. Amplitude ratios and phase shifts for the three strongest modes of XX Pyx compared with theoretically predicted values. Boundaries for the $\ell = 0$ area of interest are shown with full lines, those for the $\ell = 1$ area with dotted lines and those for $\ell = 2$ with dash-dotted lines. No meaningful result can be obtained from this diagram.

$T_{\rm eff} = 8414$ K, $\log g = 4.20$, model for a pulsation constant $Q = 0.016$ d (Fig. 12) shows obvious disagreement between the theoretically predicted values and the observations.[4] We therefore advise against the use of the information in Table 5 for mode identification at face value. We cannot say whether the disagreement is due to systematic errors in the determination of the amplitude ratios and phase shifts or due to a problem of the method itself.

Assuming the latter to be true, we can gain some understanding when recalling the principles of this mode identification technique. As mentioned above, it relies on the fact that the amplitude and phase at a given passband depends on the spherical harmonic degree, ℓ (see, for example, Balona & Evers 1999). The dependence is due to the geometric variation and the integral of the limb darkening. The limb darkening term is, however, of little importance in determining the amplitude and phases. The gravity and temperature variations do not depend on ℓ (Balona & Dziembowski, private communication). Furthermore, the temperature term is always larger than the geometric term and rapidly dominates as the period decreases, since it is proportional to the square of the pulsational frequency. This means that the dependence of the amplitudes and phases on ℓ diminishes very rapidly for higher-order p modes. For XX Pyx which is on the main sequence and has such p modes excited, the amplitudes and phases are practically independent of ℓ. The photometric method of mode identification therefore fails in this case.

6 DISCUSSION OF THE AMPLITUDE AND FREQUENCY VARIATIONS

One of the results of Section 4.3 was that three modes were variable in amplitude and phase during the observations; five more modes appeared to show amplitude variations only. In the following, we would like to comment on this result and its implications.

First of all, it must be pointed out that some of the five modes for which only amplitude variations were reported may be variable in frequency as well, but our data set is not sufficient to prove this. Some of these modes have low amplitude; phase determinations are therefore not well constrained. Second, it is now clear that the analysis of the amplitude and frequency variations of XX Pyx by HPZ can only be taken as a guide towards the long-term behaviour of this star's modes. The variability we found in the present paper is generally smaller in amplitude, but the time scales are shorter; the data set of HPZ is insufficient to sample these variations adequately. In any case, it appears pointless to attempt assigning one certain time scale to the observed variations, although approximate time-scales should be discussed.

Starting with the three modes that are variable both in amplitude and phase, we need to say that the time scales of both variations are the same (within the errors of determination) for two modes (f_2 and f_3), but they are vastly different for f_4. The latter mode also shows the largest relative amount of variability, both in amplitude and phase. On the other hand, the amplitude variability of f_2 seems to be the most complicated of all modes.

Concerning the modes examined in Fig. 7, it is also evident that not all amplitude variations necessarily contain a short-term cyclic component with a time scale shorter than the length of our data set. Some amplitudes just seem to change slowly in time. For some modes with cyclically variable amplitudes it appears that the amplitude of these variations is not necessarily constant (e.g. f_6).

Finishing our description of the observed behaviour, we consider the variability time-scales of all modes with cyclic amplitude variations. It seems that they are all about the same (except for f_4 and maybe f_{12}). How does all that relate to the results of HPZ?

The diverse behaviour of the different modes rules out any presently known explanations for the cause of the amplitude and frequency variability, except resonances between the modes (see HPZ for more detailed arguments). In this case one would expect amplitude modulations with a time-scale of the order of the inverse growth rates of the modes. HPZ examined that possibility and suggested it is consistent with the observations, within the uncertainties of the observations and of the growth rates (there is no unique model for XX Pyx yet). One quantitative statement can, however, be added now: the growth rates of the pulsation modes of the models depend on frequency (e.g. see fig. 5 of HPZ). For models of XX Pyx, this means that the growth rates for modes near 320 μHz are much smaller than those for modes around 420 μHz (0.3 versus 8 $\rm yr^{-1}$ for the specific model used by HPZ). However, the time scales of the amplitude variations of the star are not consistent with this picture; they do not show a frequency dependence. The hypothesis of resonances being responsible for the amplitude and frequency variations is however not invalidated: a suitable choice of parameters for model calculations might be able to reproduce the observed behaviour. The major drawback of this hypothesis therefore manifests itself: it is extremely difficult to verify observationally. Finally, we should add that theoretical growth rates for mixed modes are quite different from those of pure p-modes, which could also at least partly be responsible for the apparent disagreement between observations and theory.

XX Pyx is not the only δ Scuti star with well-documented temporal variability of its pulsation spectrum: the star 4 CVn has been observed for more than 30 yr. The amplitude variations of 4 CVn have most recently been described by Breger (2000). Regrettably, possible frequency variability could not be examined reliably because of large gaps in the data. We can therefore only compare the amplitude variations of the two stars. Those of 4 CVn seem to occur on much longer time scales (we caution again that the data set for this star contains large gaps, as did that of HPZ; therefore some variations could be undersampled) than those of XX Pyx. Therefore, no repeated cycles can yet be seen in the amplitude variations of 4 CVn. Still, some features are similar in principle: there is no obvious correspondence between the behaviour of the different modes, and it is also hard to define a single characteristic time scale on which the variations of the individual modes occur.

In addition, 4 CVn also shows one mode whose variations are more dramatic than all the others, similar to our f_4. This mode of 4 CVn also showed an apparent phase jump by 180°. We note for completeness that we also observed this for some weak modes of XX Pyx, but because these phase jumps occurred at very low amplitude, the corresponding errors in phase determination are large and this led us to doubt the reality of such features.

We finally mention that Breger (2000) noticed that the most unstable mode of 4 CVn also generates the largest number of combination frequencies, which he took as support for the idea that the amplitude variations are caused by transfer of energy between the modes. This is not the case for XX Pyx, where the presence of combination terms rather seems to be dependent on the amplitude of the parent modes. As a matter of fact, no

[4] It could be suspected that the signs of the observed phase shifts are wrong. This is not the case.

(possible) identification of the combination frequencies of XX Pyx involves the most variable mode, f_4. We do not wish to comment further on this topic as the exact physical nature of the combination frequencies is far from being understood, which will make any statement relying on these features highly speculative.

7 SUMMARY AND CONCLUSIONS

The 17th run of the Delta Scuti Network, devoted to the unevolved pulsator XX Pyx, resulted in the largest single data set ever reported for a pulsating star other than the Sun: 550 h of multisite measurements obtained in 125 clear observing nights at eight different sites. Both photomultiplier and CCD detectors were employed; filters were selected to take advantage of their different wavelength sensitivities.

As a first result, our data analysis revealed two new variable stars in the fields of some of the CCDs used. Turning to the programme star, we found the frequency analysis of its time-series photometric measurements disturbed by amplitude and frequency variations occurring during our observations. We developed a *non-linear frequency analysis* method which was employed to take the temporal variability of the pulsation spectrum into account. We also found that noise correlation leads to error estimates in frequency, amplitude and phase that are approximately a factor of two higher than their formal values. Finally, we were able to detect 22 independent mode frequencies for XX Pyx, which is the most ever found for a δ Scuti star. In addition, eight combination frequencies were revealed. Compared to previous work on the star, we therefore increased the number of pulsation frequencies by nine and the number of combination frequencies by eight.

We found a preferred frequency separation within the pulsation modes, confirming the result originally published by HPO. Having now almost twice as many mode frequencies available, we find that their values show clear patterns as well: they consist of distinct groups of closely spaced modes. These results lead to a refinement of the mean density ($\bar{\rho} = 0.241 \pm 0.008\,\bar{\rho}_\odot$) and to a new constraint on the rotation rate of XX Pyx ($\nu_{\rm rot} = 1.1 \pm 0.3\,{\rm d}^{-1}$). Attempts to identify the modes by pattern recognition failed. In addition, potential mode diagnostics obtained by the analysis of our colour photometry failed as well. Consequently, asteroseismology of the star requires detailed model calculations.

The diverse behaviour of the amplitude and frequency variations of some of the modes leaves resonances as the only plausible possibility for their explanation. We attempted to point out possible inconsistencies of the observations with the predictions of this theory, although we are aware that it is difficult to conflict with observations as it has little predictive power.

ACKNOWLEDGMENTS

This work was partially supported by the Austrian Fonds zur Förderung der wissenschaftlichen Forschung under grant S–7304. TA and CS acknowledge financial support from the Belgian Fund for Scientific Research (FWO). This project was supported by the Flemish Ministry for Foreign Policy, European Affairs, Science and Technology. Perth observations were made possible by the technical expertise of Arie Verveer, technical manager at Perth Observatory, and by the continued support of the Government of Western Australia. Observations at the Wise Observatory are supported in part by the Foundation for Basic Research of the Israeli Academy of Sciences. We are grateful to Mike Montgomery for the calculation of theoretical values of amplitude ratios and phase shifts applicable to our target star. Scot Kleinman is thanked for supplying his code for automatic identification of combination frequencies. The referee, Wojtek Dziembowski, provided constructive criticism on mode identification.

This paper is based on observations obtained at McDonald Observatory, the European Southern Observatory (ESO, application 60D0148), the South African Astronomical Observatory (SAAO), Siding Spring Observatory, Perth Observatory, the Southeastern Association for Research in Astronomy (SARA) Observatory, Wise Observatory and Vainu Bappu Observatory.

REFERENCES

Arentoft T., Kjeldsen H., Nuspl J., Bedding T. R., Fronto A., Viskum M., Frandsen S., Belmonte J. A., 1998, A&A, 338, 909
Balona L. A., Evers E. A., 1999, MNRAS, 302, 349
Balona L. A., Stobie R. S., 1979, MNRAS, 189, 649
Bond H. E. et al., 1996, AJ, 112, 2699
Breger M., 1990, Commun. Asteroseismol., 20, 1 (University of Vienna)
Breger M., 2000, MNRAS, 313, 129
Breger M. et al., 1993, A&A, 271, 482
Breger M. et al., 1999, A&A, 349, 225
Dziembowski W. A., Pamyatnykh A. A., 1991, A&A, 248, L11
Dziembowski W. A., Krolikowska M., 1990, Acta Astron., 40, 19
Garrido R., Garcia-Lobo E., Rodriguez E., 1990, A&A, 234, 262
Handler G., 1994, Master's thesis, University of Vienna
Handler G., 1995, Baltic Astron., 4, 434
Handler G., 1998, Baltic Astron., 7, 227
Handler G., Kanaan A., Montgomery M. H., 1997, A&A, 324, 566
Handler G. et al., 1996, A&A, 307, 529
Handler G. et al., 1997, MNRAS, 286, 303 (HPO)
Handler G., Pamyatnykh A. A., Zima W., Sullivan D. J., Audard N., Nitta A., 1998, MNRAS, 295, 377 (HPZ)
Horne J. H., Baliunas S. L., 1986, ApJ, 302, 757
Kjeldsen H., Frandsen S., 1992, PASP, 104, 413
Kleinman S. J. et al., 1998, ApJ, 495, 424
Koen C., 1999, MNRAS, 309, 769
Martinez P., 1989, MNRAS, 238, 439
Montgomery M. H., O'Donoghue D., 1999, Delta Scuti Star Newslett., 13, 28 (University of Vienna)
Nather R. E., Winget D. E., Clemens J. C., Hansen C. J., Hine B. P., 1990, ApJ, 361, 309
Pamyatnykh A. A., Dziembowski W. A., Handler G., Pikall H., 1998, A&A, 333, 141
Renzini A., 1987, A&A, 188, 49
Scargle J. D., 1982, ApJ, 263, 835
Templeton M. R., Bradley P. A., Guzik J. A., 2000, ApJ, 528, 979
Watson R. D., 1988, Ap&SS, 140, 255
Zima W., 1997, Delta Scuti Star Newslett., 11, 37 (University of Vienna)

This paper has been typeset from a TEX/LATEX file prepared by the author.